α-particle decay of states in ^{11}C, ^{13}C, and ^{15}N near decay threshold

C. Lee,[1] D. D. Caussyn,[1] N. R. Fletcher,[1] D. L. Gay,[2] M. B. Hopson,[1] J. A. Liendo,[3] S. H. Myers,[1] M. A. Tiede,[1] and J. W. Baker[4]

[1]*Florida State University, Tallahassee, Florida 32306*
[2]*University of North Florida, Jacksonville, Florida 32224*
[3]*Universidad Simón Bolívar and I.V.I.C. Caracas, Venezuela*
[4]*University of South Florida, Tampa, Florida 33688*

(Received 20 February 1998)

α-particle decays from several excited states in ^{11}C, ^{13}C, and ^{15}N have been observed in three-body final state reactions induced by heavy-ion beams at 6.5–9.0 MeV/nucleon from the FSU Tandem/LINAC. Where possible, branching fraction estimates are made. Improvements in the energy resolution of the detection system have allowed the observation of many previously unreported α-particle decays, several new total energy width determinations, and a few new excited state energies.
[S0556-2813(98)06008-7]

PACS number(s): 23.60.+e, 25.70.Ef, 27.20.+n

I. INTRODUCTION AND METHOD

There are many excited states in $1p$-shell nuclei for which the excitation energy is above the α-particle decay threshold by 2 MeV or less. Often for these states there has been no observation of the α-particle decay and even less frequently are there determinations of the α-particle decay widths. States above and near decay threshold can be of astrophysical interest since it is in the region where a stellar Maxwell-Boltzmann distribution and narrow resonances near threshold overlap that possibly significant portions of stellar reaction rates are determined. Essential to those determinations are decay branching fractions, whether for nuclear reaction rates or compound elastic scattering rates.

The measurement of α-particle partial widths by resonance scattering at bombarding energies of a few hundred keV is often very difficult because of the intense Coulomb scattering. The method used for examining α-particle decays in this work is resonant particle decay spectroscopy (RPDS) [1]. Recoiling excited $1p$-shell nuclei are produced in heavy-ion inverse kinematics reactions. These nuclei decay in flight, sometimes no more than 100 nuclear diameters from the reaction site, and the two fragments are detected in coincidence in x-y-position-sensitive counter telescopes or x-position-sensitive single detectors. The simultaneous determinations of the energies, masses, charge numbers, and the vertical and horizontal positions of decay fragments in the counter telescopes, along with careful calibrations, allow the experimenter to extract the three-body final state Q value, the decay energies, and the α-particle decay angles relative to the beam axis or the excited state nuclear recoil axis. Our previous work on ^{15}N* decay [2,3] has demonstrated that RPDS can be an effective tool for extracting α-particle branching fractions in a fairly model-independent manner. The work of Ref. [2] produced agreement in the α_0-branching fraction for the 11.44 MeV, $j^\pi = 7/2^-$ state in ^{15}N with the work of Wang *et al.*, who conducted a difficult study of low-energy resonance reactions [4].

The current work reports an investigation of α-particle decays in the reactions initiated by ^{6}Li plus 65 MeV ^{10}B, ^{7}Li plus 58.5 MeV ^{9}Be, and ^{7}Li plus 90 MeV ^{12}C. Previously unreported α-particle decays are observed in ^{11}C*, ^{13}C*, and ^{15}N*, and the last two are investigated with much improved decay energy resolution.

II. EXPERIMENTAL DETAILS

The nature of our application of the RPDS method has been explained in great detail in our previous work [2,5]; however, it will be useful to review the different detector geometry employed in the current experiments. The detector array consists of three detector positions. The first detector, centered at 9° beam left, is an x-y-position-sensitive counter telescope with a 33 μm thick DE detector and a 1000 μm thick E detector. Each detector has an active surface area of 12 mm$\times$12 mm as do the detectors of counter telescope 2, which is centered at 17° beam left. This second counter telescope employs a 67 μm thick DE detector and is otherwise identical to detector 1. Detector 3 is a single 1000 μm thick detector, 50 mm$\times$10 mm in area, with position sensitivity in the longer, horizontal, dimension. It is centered near 33° beam left. All target to detector distances, approximately 150 mm, are known to better than 1 mm. Detector angles are known to $\pm 0.05°$. These accuracies are important for reliable reconstruction of the three-body final state kinematics. In the detection of α-particle decays of a recoiling nucleus, the energy of the heavy fragment and its x-y position relative to the detector center are identified in detector 1, while the energy and position of the α-particle are determined in either detector 2 or 3. Position measurement in the y (out-of-plane) direction is unnecessary for detector 3, since this detector is sufficiently far from detector 1 that the y coordinate of the α-particle does not significantly influence the decay angle between the two detected fragments. Blocks of coincidence data will be referred to as 1-2 or 1-3 coincidence according to the detector pairs involved.

There is also a target monitor detector above the horizontal reaction plane, at 16° from the beam axis. Energy loss of the beam in the target is measured by an in-beam gold secondary target and detector arrangement, which is located

about 40 cm beyond the primary target. The combination of these two monitoring systems allows the experimentor to make rough but quantitative determinations of carbon buildup and oxidation on the primary target during the actual experiment.

In all experiments, the singles count rate in detector 1 is held to 5 kHz or less to keep the true to accidental coincidence ratio greater than 10 and to limit the count rate dependence of position resolution which has been shown [6] to rapidly deteriorate for count rates exceeding 6 kHz. With target areal densities of the order of 200 $\mu g/cm^2$, this required beam currents of the order of 10 nA or less.

III. DATA AND DISCUSSION

A. Decay of ^{11}C from the reaction ^{6}Li(^{10}B,^{11}C*)

In an early attempt to observe α-particle decay of ^{13}C, we bombarded a ^{6}Li target with 65 MeV ^{10}B beam particles. The resulting coincidence *E-DE* spectra showed clear separation of ^{6}Li and ^{7}Li ions as well as ^{7}Be and ^{9}Be ions in detector 1, while in detector 2, there was a clear separation of α, ^{6}Li, and ^{7}Li ions. We were seeking to identify the ^{6}Li(^{10}B,^{13}C*$\rightarrow\alpha+^{9}$Be)^{3}He reaction. When the data were analyzed there was no evidence for $\alpha+^{9}$Be coincidence events. This implies that not only is there no significant formation of ^{13}C* which decays by α-particle emission, but also there is no significant direct three-body final state formation of $\alpha+^{9}$Be$+^{3}$He.

On the other hand, the coincidence events of $\alpha+^{7}$Be show clear evidence for the α decay of ^{11}C*. A spectrum of contributing three-body final state Q values is generated by calculating, event by event, $Q=E(\alpha)+E(^{7}\mathrm{Be})+E(^{5}\mathrm{He})-E(^{10}\mathrm{B})$, where $E(\alpha)$ and $E(^{7}\mathrm{Be})$ are measured energies, $E(^{5}\mathrm{He})$ is calculated by use of conservation of momentum, and $E(^{10}\mathrm{B})$ is the energy of incident ^{10}B particles at the center of the target. In this spectrum there is a clearly identifiable peak at $Q=-3.51$ MeV corresponding to the three final state particles (^{7}Be,α,^{5}He) in their ground states, but it is not easily separated from the contributions from ^{5}He and its excited states, primarily due to the widths of the ^{5}He states. The four-body Q value, representing $2\alpha+^{7}$Be$+n$, has a threshold at $Q=-2.62$ MeV and its contribution to the generated spectrum extends to much more negative values in a continuum due to the fact that only two of the four particles are being detected. The contribution uncertainties are partially clarified by constructing an event-by-event two-dimensional plot of the calculated Q value vs the relative energy between the detected α particle and ^{7}Be, i.e., the decay energy of ^{11}C*. Upon inspection of such a plot it becomes very clear that there is no α-particle decay of ^{11}C* to excited states of ^{7}Be. In addition the Q-value continuum is due to a combination of final state sequential decays ^{11}C*$+^{5}$He*$\rightarrow\alpha+^{7}$Be$+^{5}$He* and the 4 MeV width of the first excited state of ^{5}He, and a direct three-body component which still involves ^{11}C* decay, i.e., ^{11}C*$+\alpha+n\rightarrow^{7}$Be$+2\alpha+n$.

The events from the Q spectrum gated on the ground state region are used to generate the ^{11}C*$\rightarrow\alpha+^{7}$Be decay angle and decay energy data shown in Figs. 1 and 2. Differences in energy resolution and calibration between the regions for

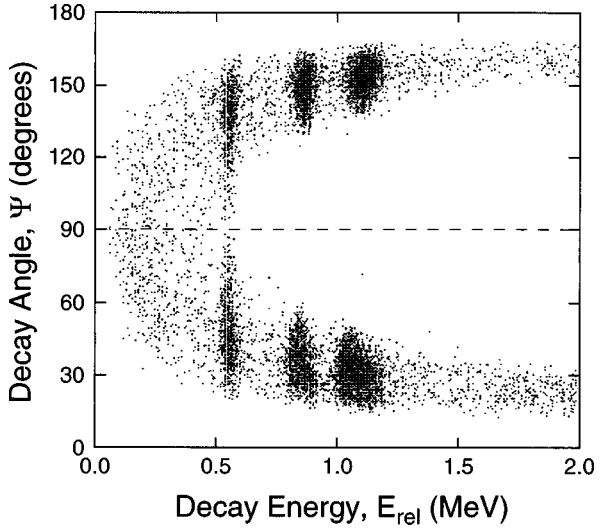

FIG. 1. Event plot of ^{11}C* decay energy vs the α-particle decay angle measured from the ^{11}C* velocity direction. The detection threshold is about 50 keV above the decay threshold.

$\psi\leqslant 90°$ and for $\psi\geqslant 90°$ in Fig. 1 are due to the fact that energy calibrations were done for the energy range and particles anticipated for ^{13}C* decay. From Fig. 1 it can be inferred, and it is verified quantitatively with simulation calculations, that the detection efficiency for the formation and decay for the excited states of ^{11}C has a maximum in the neighborhood of 300 keV above the decay threshold and from there it decreases monatonically as the decay energy increases. The observed three states of ^{11}C are well known [7]. Since the system efficiency is decreasing with decay energy, it is clear that the double differential cross section for the formation and subsequent α-particle decay of these three states is increasing rapidly with excitation energy. It abruptly falls to near zero for all ^{11}C states at an excitation energy higher than the 8.65 MeV state.

The branching fractions Γ_{α_0}/Γ for the 8.10 MeV and 8.42 MeV excited states in ^{11}C are $\sim 0.6\pm 0.4$ and 0.8 ± 0.2, respectively [7], as determined from the resonance reaction ^{7}Be(α,γ). It is unfortunate that we are unable to determine the branching fractions directly by the method of Liendo *et al.* [2], but that would require the measurement of the ^{11}C* production cross section in the reaction ^{10}B(^{6}Li,^{5}He)^{11}C*, which is not possible due to the extremely short lifetime of ^{5}He.

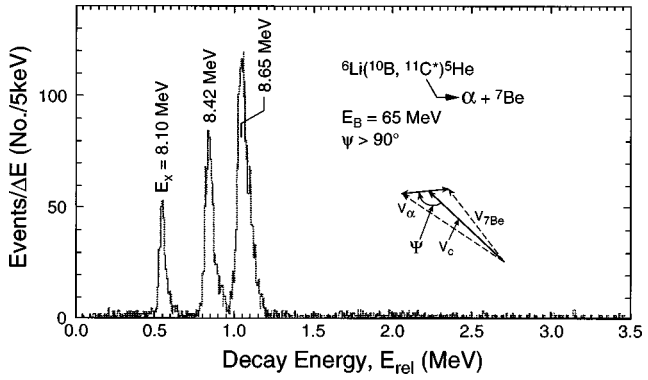

FIG. 2. Decay energy spectrum for ^{11}C*$\rightarrow\alpha+^{7}$Be(g.s.) produced at 65 MeV ^{10}B bombardment of ^{6}Li.

TABLE I. Decay branching fractions in ^{11}C*.

$E_x(^{11}\mathrm{C})$ (MeV)	Γ_γ/Γ [a]	$\Gamma_{\alpha_1}/\Gamma_{\alpha_0}$ [b]	Γ_{α_0}/Γ [c]
8.105	0.03 ± 0.02	$\leqslant 0.03$	0.97 ± 0.03
8.420	0.20 ± 0.10	$\leqslant 0.01$	0.80 ± 0.10
8.655	Not observed	$\leqslant 0.01$	~ 1.00

[a]From Refs. [7] and [8].
[b]Present work for α_0 and α_1 decays.
[c]Combined result of Refs. [7,8], and present work.

The previously determined branching fractions Γ_{α_0}/Γ had large errors since, being measured in the (α,γ) reaction, there was no knowledge of the α_1-decay branch, which is the only other channel open. In the present experiment we can determine upper limits on the α_1 decay from the previously mentioned E_{rel} vs $-Q$ spectrum, since the α_1-decay energies conveniently fall at barren regions of the relative energy spectrum. For all three states observed, the detection efficiency for $\alpha_1+{}^7$Be* decay is greater than for the corresponding $\alpha_0+{}^7\mathrm{Be}_{\mathrm{g.s.}}$ decay since the former represents lower decay energies. This fact further decreases the lower limit we can place on the α_1 decay of ^{11}C*. We conclude that $\Gamma\alpha_1/\Gamma\alpha_0$ is less than 3% for the state at $E_x=8.105$ MeV and less than 1% for states at 8.425 and 8.665 MeV. Therefore essentially all of the natural width not in the γ decay channel is in the α_0-decay channel. These results are summarized in Table I. The small α_1 branch for these three states can be anticipated since, in each case, the minimum allowed l value for α_1 decay is greater than or equal to that for the higher-energy α_0 decay.

All states at higher excitation energy appear to have a near zero double differential cross section for the formation of ^{11}C* and its α decay. The decay channel for proton emission from ^{11}C opens at 8.69 MeV, and even though the next two higher-energy excited states of ^{11}C have large spin ($j^\pi=5/2^+$), a low energy $l=0$ proton decay is allowed due to the $j^\pi=3^+$ for the ground state of ^{10}B, thus effectively quenching any possible α-particle decay for these higher-energy excited states of ^{11}C.

B. Decay of ^{13}C* from the reaction ^{7}Li(^{9}Be,^{13}C*)

The α-particle and ^{9}Be decay products from excited states of ^{13}C*, which were produced by bombardment of a ^{7}Li target by 58.5 MeV ^{9}Be particles, have been observed in coincidence detector pairs 1-2, and 1-3. Detector 1 was calibrated in energy and position by use of ^{9}Be particles whereas detector 2 and the 5 cm long detector 3 were calibrated by use of the α-particle emissions from a ^{228}Th source. With typically five calibration energies and nine calibration positions, the rms deviations from the low-order polynominal calibration functions are listed in Table II.

Reconstructed negative Q spectra for the $^9\mathrm{Be}+\alpha$ coincidences and the assumed three-body final state of $^9\mathrm{Be}+\alpha+t$ are shown in Fig. 3. The peak at the anticipated value of $Q=-2.47$ MeV is clearly visible; however, the yield is weak and a clear separation of this peak is hindered by considerable background. A number of investigations have been made into the nature of this background. In two-dimensional spectra of three-body Q value vs time of flight, we do observe contributions from accidental coincidences from different beam pulses (every 20 ns); however, that contribution is less than 15% of the background of Fig. 3. Also the ''true'' coincidences of the Q peak are slightly separated in time from the background, but not sufficiently to eliminate it through a time gate.

TABLE II. Detector center angles and calibration standard deviations for energy and position measurement.

Laboratory angle ($\pm0.05°$)	Detector	rms of energy (keV)	rms of position (mm)
9.05°	DE_1	9.72	0.064
	E_1	15.64	0.049
17.05°	DE_2	2.16	0.008
	E_2	8.93	0.030
32.63°	E_3	5.47	0.212

The elemental content of the target has been analyzed for a possible contribution to the background, since if a different mass of the third particle is incorrectly assumed to be that of the triton, then the resulting contribution to the Q spectrum will acquire great width and possibly appear to be a continuum. The double monitor technique is very valuable for this analysis. By elastic scattering of 30 MeV ^{16}O into the 16° out-of-plane monitor we clearly separate target constitu-

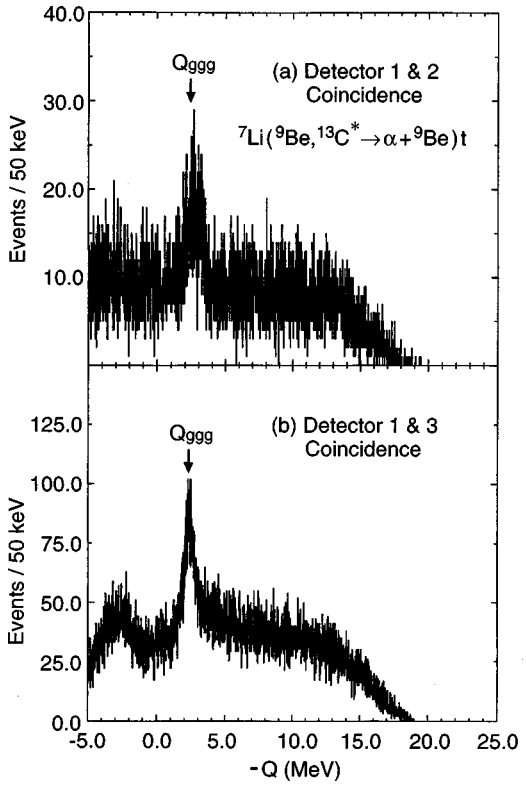

FIG. 3. Spectra of Q values generated event by event for 1-2 and 1-3 coincidences from $^{13}\mathrm{C}^*\rightarrow\alpha+^9$Be. The Q_{ggg} arrow represents the Q value calculated from mass differences for all the three final state particles in their ground state.

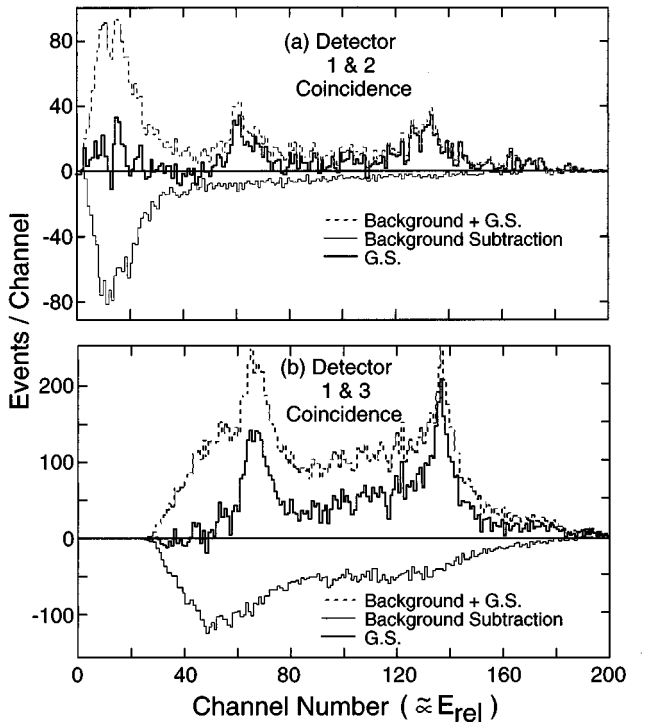

FIG. 4. Spectra of relative energy between coincidence detected particles, α and ^{9}Be, when the data of Fig. 3 are gated on the ground state Q peak (dashed histograms) and gated off the peak to indicate the background spectra (solid histograms shown negatively). The difference spectra (positive solid histograms) indicate decay energies for $^{13}C^{*}\rightarrow\alpha+^{9}$Be(g.s.).

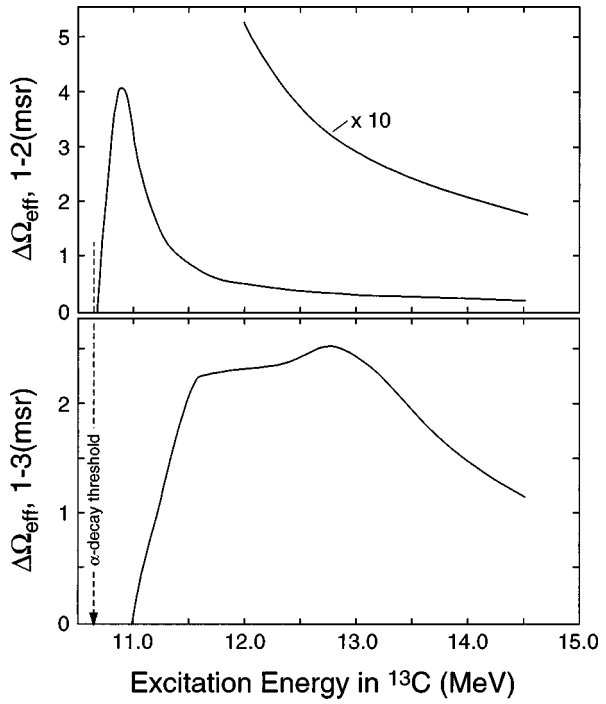

FIG. 5. Results of Monte Carlo simulations of the effective solid angle $\Delta\Omega_{\rm eff}$ for the detection of $^{13}C^{*}$ through its α-particle decay in the reaction ^{6}Li(^{10}B,$^{13}C^{*}\rightarrow\alpha+^{9}$Be)$t$ at $E(^{10}\mathrm{B})=65$ MeV.

ents of ^{7}Li, ^{12}C, and ^{16}O. When the data of Fig. 3 are analyzed as ^{9}Be-induced reactions on ^{12}C or ^{16}O, no appreciable component of the background coalesced into Q peaks representing reactions on these known target impurities, thus eliminating this possible source of the background in the spectra of Fig. 3.

This particular reaction is the first time we have attempted to study α decay resulting in a three-body final state that could also be formed by direct breakup of a beam or target particle, and it has resulted in a background contribution which could not be eliminated in a systematic fashion. In reality, however, the problem is not high background, but rather a low yield for the formation and decay of $^{13}C^{*}$, even though we have employed a high-efficiency detection system. When compared with our previous work [2] which had comparable detector count rates, our current background counts per energy interval in the Q spectrum are actually less by more than a factor of 2 while the Q_{ggg} yield for 1-2 coincidence is down by a factor of 40. Our remaining alternative to deal with this low signal-to-background ratio is the formation of the relative energy ($E_{\rm rel}=$ decay energy) spectra for data gated on the Q peak (Fig. 3) and on either side of the Q peak and then performing background subtraction. The result of this procedure is shown in Fig. 4. The back ground contributions, illustrated as negative histograms, show a strong enhancement at low relative energy between the α-particle and the ^{9}Be, especially for the 1-2 coincidence which has a high efficiency at low relative energy. The high-decay-energy portion of the spectrum of Fig. 4(a), greater than channel 100, has very little background contribution for 1-2 coincidence data, but background still accounts for nearly half of the total yield for 1-3 coincidences, the spectrum of Fig. 4(b), where at high relative energy the detection efficiency is much greater. The energy dependences for the 1-2 and 1-3 effective solid angles for the detection of $^{13}C^{*}$ decay in this experiment are shown in Fig. 5.

The solid positive histograms of Fig. 4 represent decay energy spectra for α-particle decays of $^{13}C^{*}$ to the ground state of ^{9}Be. In Fig. 6, we have displayed these same spectra with Gaussian representations of peaks which correspond to many known excited states in ^{13}C. The energy labels in Fig. 6 are the previously reported energies from Ref. [9]. The presently observed excitation energies and energy widths are compared to previous information in Table III. The apparent yield between channels 30 and 50 for 1-2 coincidences in Fig. 6 can be seen from Fig. 4(a) as statistical fluctuations about zero, and indeed there are no known ^{13}C excited states in this region. However, a similar yield above channel 150 represents real decay information since here the background is near zero.

The ^{13}C excited states listed in Table III are numbered to facilitate discussion. The excitation energies from the current work are calculated from our detector calibration as $E_x=C\times 0.02$ MeV$+E_{\rm th}$, where C is the Gaussian centroid and $E_{\rm th}$ is the decay threshold energy, 10.648 MeV. There is general agreement between our experimentally determined values and those listed in Ref. [9] for the states numbered 1, 2, 3, 4, 6, 10, and 14. The first two states represent the lowest α-particle decay energies ever observed from excited states. Newly adopted excitation energies or widths based on the current work are listed in the far right of Table III. States 5 and 7 which are clearly observed in Fig. 6, especially in the 1-3 coincidence, have considerably narrower widths than previously presented. The broad state, No. 8, is given a width

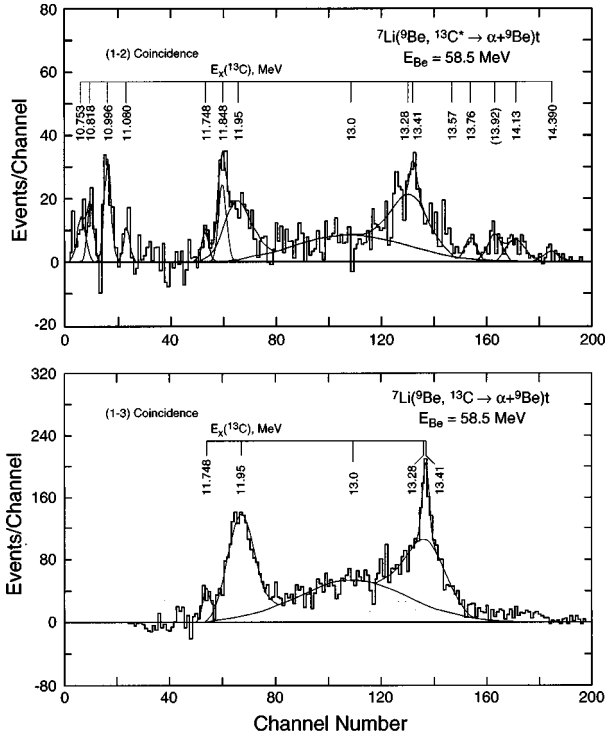

FIG. 6. α-particle decay energy spectra for excited states of ^{13}C. Excitation energies shown are from Ref. [9]. Centroids (Ch.#) of Gaussian curves give excitation energies from this experiment as E_x(MeV) = 10.648 + (Ch.#) × 0.020. Comparisons are shown in Table III.

of 1000 ± 200 keV and is positioned at 12.8 MeV ± 200 keV in the present work. Recall that the Gaussian curves in Fig. 6 are located at the E_x values of the present work although their labels in Fig. 6 are from Ref. [9]. The previously uncertain state at 13.28 MeV is confirmed and a new state is proposed at 13.92 MeV. Notice that in the fitting for the 13.28 MeV state in 1-3 coincidences, Fig. 6, the region around state 11 (near channel 146) was included as part of state 9, and without that inclusion the energy and width in Table III would be 13.30 MeV and 300 keV, respectively, in good agreement with the result obtained from fitting the 1-2 coincidence data, hence the adopted values of E_x = 13.28 MeV and Γ = 310 keV. The 30 keV uncertainties for the two states, 9 and 13, are conservatively based on the fact that the rms deviation of current energies for states 1–7 plus 15 from those of Ref. [9] is 25 keV. Discrepancies remain in the widths of states 11, 12, and 15. In each case the current widths are considerably less than those listed in Ref. [9]; however, our yields are very small and state 11 (near channel 146) is not included in the fitting of Fig. 6.

Clearly, the yields for ^{13}C* α-particle decay are too small to form decay angular correlations and therefore double differential cross sections for the formation and decay, as was done for ^{15}N* in Ref. [2]. The utility of that method is to obtain model-independent determination of α-particle branching fractions. Even with the small yields, an estimate of branching fractions could be made if one had a measurement of the formation differential cross sections for the reaction ^{9}Be(^{7}Li,t)^{13}C*. This requires detection of relatively high-energy tritons with an energy resolution of 50 keV or better which would probably require the use of a magnetic spectrograph.

C. Decay of ^{15}N* from the reaction ^{7}Li(^{12}C, ^{15}N*)

Our previous work on the formation and α-particle decay of ^{15}N* has indicated the possibility of new excited states [10,11] and very narrow widths for the excited states at 12.55 and 13.00 MeV [2]. We have conducted a repeat experiment in order to obtain better $E_{\rm rel}$ resolution by use of the current 1-2 detector geometry at 150 mm from the target as opposed to the earlier approximate 1-3 geometry at 100 mm from the target. Again the bombarding energy was 90 MeV. Gating on a well-formed peak in the Q spectrum corresponding to the three-body final state of ^{11}B$_{\rm g.s.}$ + 2α, we obtain the $E_{\rm rel}$ spectrum shown in Fig. 7 with an energy resolution of 70 keV at 12.55 MeV excitation, improved from the previous 120 keV. Because of energy loss effects for ions exiting from the target, it is well known that a better energy resolution is observed when spectra are gated on relatively narrow ranges of formation and decay angles. Examples of such spectra are shown in Fig. 8 for the excitation energy region near the strong states at E_x = 12.55 and 13.00 MeV. Here we observe a system resolution of about 40 keV compared with 90 keV from the earlier work.

The excitation energies extracted from a Gaussian fitting of these spectra are shown in Fig. 8, and are compared with values from Ref. [9] in Table IV. Current values are calculated from $E_x = C \times 0.01 + E_{\rm th}$, where C is the peak centroid and $E_{\rm th}$ is the α-decay threshold, 10.992 MeV. Width information is not included in Table IV since, unlike the ^{13}C case, in ^{15}N we are not dealing with any known widths significantly greater than the experimental energy resolution. Widths of 7 ± 3 keV are reported for the states at E_x = 13.15 and 13.17 MeV, and based on that we conclude that our experimental width is slightly less than 40 keV for the data of Fig. 8, since 40 keV was used for the fitting width in that region of the spectra.

Several additional states have been predicted to exist near this energy region based on a weak coupling model [12]; however, the energy correspondence between experiment and theory for these weak coupling levels is sometimes no better than an MeV [12]. The search for confirmation of possible new states between the strong states at 12.55 and 13.00 MeV, which were reported earlier [11], as possible weak coupling states, has not been successful. Although there is reasonable evidence for states near 12.62 MeV in Fig. 8(b) and near 12.87 MeV in Fig. 8(a), they are not sufficiently close in energy to similar data cited earlier, and we expected that with our improved energy resolution the peaks in question would have stood out much more clearly.

New excitations in ^{15}N are proposed for the region of 13.1–13.2 MeV. Because of the accuracy of the energy correspondence for the strong excitations at 12.55 and 13.00 MeV, we believe that the tabulated doublet at 13.149 and 13.174 MeV, for which our spectra show some unresolved evidence, is actually the excitation which we have listed at about 13.16 MeV. The triplet fitting of this region of the spectra of Fig. 8 then indicates two new excitations at 13.108 and 13.199 MeV, each with an estimated absolute uncertainty of 15 keV (see Table IV).

TABLE III. Energies and widths of excited states in ^{13}C.[a]

State	Values from Ref. [9] E_x	Values from Ref. [9] Γ	Present work (1-2) coincidence E_x	Present work (1-2) coincidence Γ [b]	Present work (1-3) coincidence E_x	Present work (1-3) coincidence Γ [b]	Proposed new adoptions E_x	Proposed new adoptions Γ
1	10.753±4	55±2	10.768 [c]	55				
2	10.818±5	24±3	10.838 [c]	25				
3	10.996±6	37±4	10.969	33±5				
4	11.088±5	<4	11.112	<15				
5	11.748±10	110±15	11.711	33±10	11.70	43±10	11.74±10	40±10
6	11.848±4	68±4	11.841	46±9				
7	11.95±40	500±80	11.959	235±40	11.969	240±30	11.96±30	240±30
	(Five states at 12.106, 12.13, 12.14, 12.187, and 12.438 MeV.)		Unobserved					
8	13.0±1000	(broad)	12.83 [d]	1000	12.83	1000	12.8±200	1000±200
9	(13.28)	340	13.27	315±30	13.36	380±40	13.28±30	310±30 [f]
10	13.41	35±3	13.30	33±10	13.37	33±10		
11	13.57	620±50	(13.53) [e]	(65)	(13.57) [e]	(85)		
12	13.76	≃300	13.73	77±30				
13			13.92	100±25			13.92±30	100±30
14	14.13	≃150	14.08	160±20				
15	14.390±15	280±70	14.36	115±35				

[a]Excitation energies are in MeV; uncertainties and widths are in keV. Uncertainties in excitation energies of the present work are <30 keV (see text).
[b]Widths shown in Fig. 6 are Γ_{expt}, while the widths listed here are $\Gamma=\sqrt{\Gamma_{\text{expt}}^2-50^2}$, taking the experimental resolution as 50 keV from state 4.
[c]Energy separation for fitting was fixed at 70 keV and Γ_{expt} was fixed at $\Gamma_{\text{expt}}=\sqrt{\Gamma^2+50^2}$, using Γ values from Ref. [9].
[d]Values not allowed to vary in fitting; errors estimated.
[e]Not included in fitting of data in Fig. 6.
[f]See discussion in Sec. III B.

This entire excitation region of ^{15}N has also been investigated via the ^{12}C(α,p) reaction with 17 keV resolution using a *QDDD* spectrograph at small angles [13]. They do not observe these two new states and nor do they observe all of the previously known states in this region. It is well known that states of more complex structure have an increased relative cross section at more backward angle observations, such as in the current experiment. The width information obtained by Brown and Kemper [13] is, however, very important to the interpretation of Fig. 8. They observe experimental widths for the 12.55 and 13.00 MeV states of a little less than 25 keV and a width of 32±7 keV for the 12.92 MeV state, in contrast to a tabulated value of 56±11 keV [9], while the relatively broad state at 12.94 MeV is unobserved in their work. In Fig. 8 our fitted widths of the 13.00 MeV state are over 65 keV; however if in the fitting

TABLE IV. Energies of excited $T=1/2$ states in ^{15}N.[a]

Values from Ref. [9] E_x	Present work $\Psi_z=105°-115°$ E_x	Present work $\Psi_z=115°-125°$ E_x	Proposed new adoptions E_x
12.493±4	12.491	12.501	
12.551±10	12.553	12.555	
	(12.628)	(12.622)	
	(12.875)	(12.845)	
12.920±4 12.940±10	} 12.930	12.907	
13.004±10	13.002	13.002	
	13.103	13.111	13.107±15
13.149±10 13.174±7	}13.155	13.161	(doublet)
	13.195	13.203	13.199±15

[a]Excitations energies are in MeV; uncertainties are in keV.

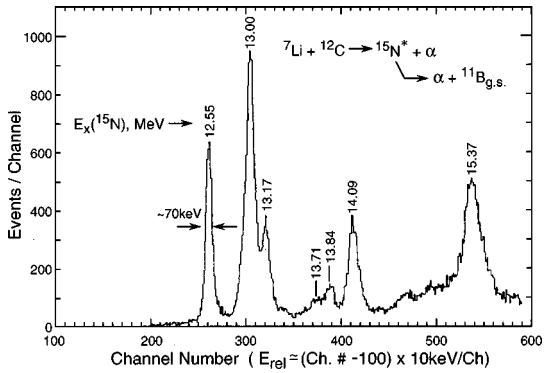

FIG. 7. α-particle decay energy spectrum from the reaction ^{7}Li(^{12}C,^{15}N*$\rightarrow\alpha+^{11}$B$_{g.s}$) at $E(^{12}\mathrm{C}) = 90$ MeV and for all formation and decay angles subtended by the 1-2 coincidence detection system. The indicated width of 70 keV represents the net experimental width when the data from all formation and decay angles are included.

we place states at 12.92 and 12.94 MeV with widths of our 40 keV experimental resolution folded into the natural widths of these states, 32 keV [13] and 81 keV [9], respectively, then not only is the fitted resolution of the 13.00 MeV state reduced to about 50 keV, but also the entire yield on the low-energy side of this strong peak is accounted for without the contribution of a state near 12.85 MeV, and all of this is accomplished with a χ^2/D value only slightly greater than that for the fit shown in Fig. 8. This result essentially eliminates further speculation on new states near 13 MeV based on the current data.

IV. SUMMARY

Our measurements show that the reaction $^{11}\mathrm{C}^*\rightarrow\alpha_1+^{10}\mathrm{B}^*$ plays no significant role in the decay of any of the three excited states of ^{11}C which lie between the decay thresholds for α-particle emission and proton emission. The current first time observation of strong α_0 decay of these states can therefore be used to determine branching fractions to a high degree of accuracy by use of the known γ-ray branching fractions.

We observe α_0 decay of 15 excited states in ^{13}C*, four of which have decay energies of less than 500 keV, and five of the excited states had never before been reported to decay by α-particle emission. Improved values for excitation energies and/or energy widths have been determined for five of the observed excited states. Branching fractions for α_0 decays cannot be determined because of unknown formation cross sections of the reaction ^{7}Li(^{10}B,^{13}C*).

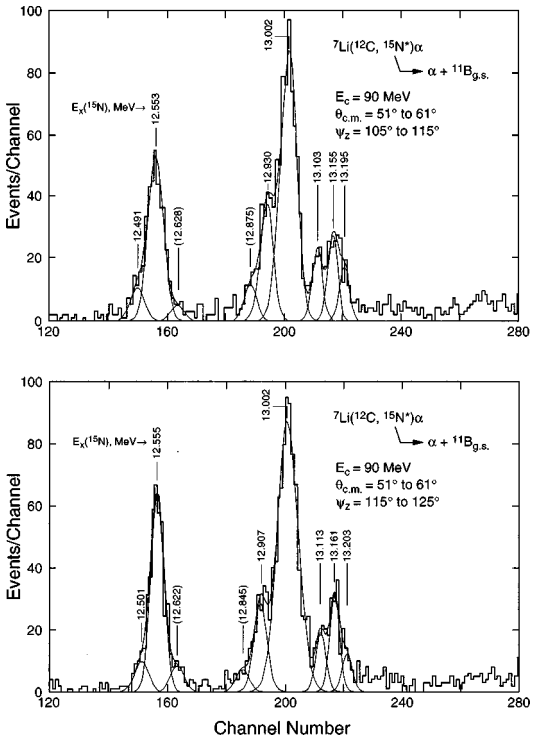

FIG. 8. α-particle decay energy spectra for excited states of ^{15}N. Excitation energies shown are from $E_x(\mathrm{MeV}) = 10.992 + (\mathrm{Ch.\#}) \times 0.010$. The energy resolution is less than 40 keV. Comparisons of excitation energies and widths with those of Ref. [9] are made in Table IV.

The high-resolution study of $^{15}\mathrm{N}^*\rightarrow\alpha_0+^{11}\mathrm{B}_{g.s.}$ has failed to verify with any statistical significance the existence of new excited states between the well-known strong states at $E_x = 12.55$ and 13.00 MeV; however new excitations are proposed at $E_x = 13.107$ and 13.199 MeV (± 15 keV), with energy widths of less than 40 keV. The α-particle decay of excitations labeled in Fig. 7 as 12.55, 13.00, and 13.17 MeV are each seen in Fig. 8 to be α-particle decay of multiplets, the latter one a quartet of states. It is clear then that the branching fractions Γ_{α_0}/Γ reported earlier [2] for these ''states'' now must be considered as average values for each multiplet.

ACKNOWLEDGMENTS

This work was supported in part by National Science Foundation Grant Nos. PHY-9523974 and INT-9401924, and NSF-REU Site Grant No. PHY-9424089. This work also received support from CONICIT (Venezuela) Grant No. PI-097.

[1] W.D.M. Rae and R.K. Bhowmik, Nucl. Phys. **A420**, 320 (1984); R.K. Bhowmik and W.D.M. Rae, Phys. Lett. **136B**, 149 (1984); S. March and W.D.M. Rae, *ibid.* **153B**, 21 (1985).

[2] J.A. Liendo, N.R. Fletcher, E.E. Towers, and D.D. Caussyn, Phys. Rev. C **51**, 701 (1995).

[3] J.A. Liendo, N.R. Fletcher, and D. Robson, Phys. Rev. C **47**, 682 (1993).

[4] T.R. Wang, R.B. Vogelaar, and R.W. Kavanagh, Phys. Rev. C **43**, 883 (1991).

[5] N.R. Fletcher, M.B. Hopson, C. Lee, M.A. Tiede, Z. Yang, and J. Liendo, Nucl. Instrum. Methods Phys. Res. A **372**, 439 (1996).

[6] Superconducting Accelerator Laboratory, Florida State University, Progress Report 1994–1997, pp. 70–74.

[7] F. Ajzenberg-Selove, Nucl. Phys. **A506**, 1 (1990).
[8] G. Hardie, B.W. Filippone, A.J. Elwyn, M. Wiescher, and R.E. Segel, Phys. Rev. C **29**, 1199 (1984).
[9] F. Ajzenberg-Selove, Nucl. Phys. **A523**, 1 (1991), pp. 17, 18 for ^{13}C; p. 119 for ^{15}N.
[10] J.A. Liendo, N.R. Fletcher, D.D. Caussyn, K.W. Kemper, and E.E. Towers, Phys. Rev. C **50**, 3155 (1994).
[11] J.A. Liendo, Ph.D. thesis, Florida State University, 1993 (unpublished).
[12] S. Lie and T. Engeland, Nucl. Phys. **A267**, 123 (1976).
[13] J.D. Brown and K.W. Kemper (unpublished).